Available online at www.sciencedirect.com
SCIENCE DIRECT®
Physics of the Earth and Planetary Interiors 151 (2005) 243–258
PHYSICS OF THE EARTH AND PLANETARY INTERIORS
www.elsevier.com/locate/pepi

Estimation of coda wave attenuation for NW Himalayan region using local earthquakes

Naresh Kumar [a], Imtiyaz A. Parvez [a,*], H.S. Virk [b]

[a] *CSIR Centre for Mathematical Modelling and Computer Simulation (C-MMACS), NAL Belur Campus, Bangalore 560037, India*
[b] *H. No. 360, Sector 71, SAS Nagar (Mohali), Ropar, Punjab 160071, India*

Received 6 October 2004; received in revised form 2 January 2005; accepted 20 March 2005

Abstract

The attenuation of seismic wave energy in NW Himalayas has been estimated using local earthquakes. Most of the analyzed events are from the vicinity of the Main Boundary Thrust (MBT) and the Main Central Thrust (MCT), which are well-defined tectonic discontinuities in the Himalayas. The time-domain coda-decay method of a single back-scattering model is employed to calculate frequency dependent values of Coda *Q* (Qc). A total of 36 local earthquakes of magnitude range 2.1–4.8 have been used for Q_c estimation at central frequencies 1.5, 3.0, 6.0, 9.0, 12.0 and 18.0 Hz through eight lapse time windows from 25 to 60 s starting at double the time of the primary S-wave from the origin time. The estimated average frequency dependence quality factor gives the relation, $Q_c = 158f^{1.05}$, while the average Q_c values vary from 210 at 1.5 Hz to 2861 at 18 Hz central frequencies. The observed coda quality factor is strongly dependent on frequency, which indicates that the region is seismic and tectonically active with high heterogeneities.

The variation of the quality factor Q_c has been estimated at different lapse times to observe its effect with depth. The estimated average frequency dependent relations of Q_c vary from $85f^{1.16}$ to $216f^{0.91}$ at 25 to 60 s lapse window length respectively. For 25 s lapse time window, the average Q_c value of the region varies from 131 ± 36 at 1.5 Hz to 2298 ± 397 at 18 Hz, while for 60 s lapse time window its variation is from 285 ± 95 at 1.5 Hz to 2868 ± 336 at 18 Hz of central frequency. The variation of Q_c with frequency and lapse time shows that the upper crustal layers are seismically more active compared to the lower lithosphere. The decreasing value of the frequency parameter with increasing lapse time shows that the lithosphere acquires homogeneity with depth.

Keywords: Coda wave; Attenuation; Lapse time; Scattering; Northwest Himalayas

1. Introduction

A seismogenic region can be characterized by tectonic, seismic and volcanic activities in addition to

* Corresponding author. Tel.: +91 80 25051 909; fax: +91 80 2522 392.
E-mail address: parvez@cmmacs.ernet.in (I.A. Parvez).

0031-9201/$ – see front matter © 2005 Elsevier B.V. All rights reserved.
doi:10.1016/j.pepi.2005.03.010

geological formation and geological history. All these properties quantify the behaviour of the seismic energy propagation in the lithosphere and can be utilized for seismic hazard mitigation. As the seismic energy propagates through the earth medium, its energy (amplitude) decays due to geometrical spreading, intrinsic attenuation and scattering attenuation. Intrinsic attenuation converts the seismic energy to heat due to anelastic absorption and scattering attenuation redistributes the energy at random heterogeneities present in the upper earth medium. Therefore, the attenuation of seismic waves in the lithosphere is an important property for studying the regional earth structure and seismotectonic activity. Jin and Aki (1988) state that the coda quality factor, Q_0 (inverse of seismic attenuation factor) at a frequency of 1 Hz can be useful to quantify the seismicity of regions. Jin and Aki (1989) strongly correlated the coda-Q^{-1} with the degree of fracture in the lithosphere associated with the seismicity.

After the advent of coda wave theory (Aki, 1969), these short-period secondary waves are utilized for crustal studies near the source in a laterally heterogeneous upper lithosphere, the seismicity of the region and earthquake source mechanism. In the single-scattering model, the coda is considered as a superposition of back-scattered wavelets from randomly distributed heterogeneities (Aki, 1969; Aki and Chouet, 1975; Rautian and Khalturin, 1978). The scattering is produced by irregular topography, complex surface geology, heterogeneous elastic property of the rocks, faults and cracks, which are more near the surface and less in the deep region. The spatial variation of regional coda quality factor has been utilized for a better understanding of tectonics, seismicity, seismic risk analysis and engineering seismology (Singh and Herrmann, 1983; Jin and Aki, 1988). It has been observed that the coda spectrum of small earthquakes for near source is independent of earthquake size, epicentral distance and the path between station and epicentre but depends on lapse time from the origin time of the earthquake (Aki and Chouet, 1975; Sato, 1977). This suggests that the coda part of the seismogram is due to an average scattering effect of the medium in the region near the source and station.

Aki and Chouet (1975) proposed two extreme models for back-scattered waves to calculate the coda quality factor, Q_c. The first single scattering model considers the scattering as a weak process without loss of seismic energy by scattering and in the second one the seismic energy transfer is considered to be a diffused process. The single scattering or multiple scattering model has been used to observe Q_c in different regions of the world (Aki and Chouet, 1975; Sato, 1977; Roecker et al., 1982; Pulli, 1984; Wu, 1985; Jin and Aki, 1988, 1989; Havskov et al., 1989; Ibanez et al., 1990; Pujades et al., 1991; Canas et al., 1991; Akinci et al., 1994; Latchman et al., 1996; Zelt et al., 1999) to observe the ongoing seismic activity and polarize the active regions from the stable regions. These studies generally show low value of Q_0 (e.g. <200) for tectonic and seismic active regions, high Q_0 value (e.g. >600) for seismic inactive stable regions and intermediate value for moderate regions. Pujades et al. (1991) described that Q_c observed by single scattering model is mainly the intrinsic quality factor Q_i, due to attenuation of only back-scattered waves, while Gao et al. (1983) suggested a multiple scattering model for primary as well as secondary waves to estimate both Q_i and Q_s (scattering) quality factors, but it is significant mainly for long (>100 s) lapse times. Sato (1988) emphasised that the single scattering model is valid even for longer lapse times. The practical problem in the multiple scattering model is to include the effect of Q_i and Q_s separately to observe the attenuation, while in coda Q, these must be observed simultaneously. Wu and Aki (1988) suggested that simultaneous estimation of Q_i and Q_s for coda may lead to unacceptably large errors for both parameters. Therefore, the single back-scattering model is preferred for coda Q calculation and according to Jin and Aki (1989), the first-order Born approximation of this model includes both the attenuation due to intrinsic absorption and the loss due to scattering. In the present paper, the single scattering model has been used to study the coda attenuation in NW Himalayas and different lapse time envelopes are taken to observe multiple scattering effects (Peng et al., 1987; Su and Aki, 1990).

The coda Q has also been estimated at different parts of India by Gupta et al. (1995) for Garhwal Himalayas, Mandal and Rastogi (1998) for Koyna region, Gupta et al. (1998) for Koyna region, Tripathi and Ugalde (2004) for southern India and Mandal et al. (2004) for Kutch area. The estimated values of Q_c are almost same for these regions but Q_0 and frequency parameter are variable with seismic, tectonic and geological features. The NW Himalayas is the seismic and tec-

tonically active region. Prominent past earthquakes of the region, are the great Kangra earthquake (1905), the Kinnuar earthquake (1975), Dharamshala earthquakes (1978, 1986), the Sundernagar earthquake (1997) and some other earthquakes of 1945, 1947 and 1950. So far, not much work has been done for seismic wave attenuation in this region, therefore, it is necessary to study the attenuation of seismic energy. This work may be useful for other research mainly in earthquake hazard assessment.

2. Tectonic setting and seismic activity

The Himalayas is the youngest mountains range formed by the convergence of the north dipping Indian plate under the southward movement of the Eurasian plate. High levels of tectonic activity resulted due to these opposite convergence movements, which have developed ISZ (Indian Tsangpo-suture zone), MCT (Main Central Thrust), MBT (Main Boundary Thrust) and HFT (Himalayan Frontal Thrust) as prominent thrusting (faulting) boundaries in the Himalayas in addition to many localized thrusts, faults, folds and minor lineaments. In the present study region, along with MCT, MBT and HFT the Jawalamukhi thrust (JMT), Drang thrust, Panjal thrust, Vakirata thrust, Sundernagar fault, Kistwar fault and Ropar fault are well known tectonic features. The tectonic movement of NW Himalayas and prominent discontinuities are shown in Fig. 1.

The MBT was formed as a normal fault during an extensional phase in NW Himalayas, prior to the Himalayan orogeny (Dubey et al., 2001). The reactivation of MBT and HFT during the Quaternary has been inferred from a variety of geological features, which is still active. Subsequent evolution of the foredeep marked by intra-basin boundary faults during this period reveals that the Himalayan foothill region has been experiencing neotectonic activity. In NW Himalayas the thrust faulting with strike-slip motion along gently dipping planes towards north, southwest and southeast have been observed from the fault plane solutions by Ni and Barazangi, 1984. The reverse faulting focal mechanism indicates that the Indian plate underthrusts the Eurasian plate at a shallow angle in the NS to NNE-SSW direction and there is a surface of decollment at which most of the seismicity concentrates. The depth of decollment is about 15 km and in the present study about 60% seismic activity has been observed around this depth. The tectonic features of NW Himalayas have been shown in Fig. 1, in which the direction of shortening in Quaternary period is indicated by a black arrow and azimuth of in situ stress are indicated by white arrow. It is clear from the figure that the major tectonic thrusts are EW and minor faults are oblique to these thrusts and support NS underthrusting of the Indian plate. Integrated fault surface area of earthquakes (Rao et al., 2003) suggest that in the NW Himalayas the seismicity is dominated by reverse faulting (93%), while in adjoining region of Tibetan plateau the reverse-faulting is a mere 2% and is dominated by strike-slip and normal faulting (59 and 39%, respectively). The region has experienced micro, moderate and high-sized shallow focus (mainly $10 \leq h \leq 20$ km) seismic activity (Ni and Barazangi, 1984). Past and present studies in this region explore the high seismic activity in Chamba-Dharamshala region between MBT and MCT.

3. Coda *Q* calculation

The coda waves have been estimated as a superposition of secondary waves through single back-scattering of primary body waves at randomly distributed heterogeneities (Aki, 1969; Aki and Chouet, 1975). The decrease of coda wave amplitude with lapse time at a particular frequency is only due to energy attenuation and geometrical spreading but independent to earthquake source, path propagation and site amplification (Aki, 1969). The attenuation of seismic waves is the sum of intrinsic and scattering attenuation, where in the first case the energy is converted to heat through anelastic absorption and in second case it is redistributed through refraction, reflection and diffraction at random discontinuities present in homogeneous medium. Generally, the Q factor increases with frequency (Mitchell, 1981) through the relation

$$Q = Q_0 \left(\frac{f}{f_0} \right)^n$$

where Q_0 is the quality factor at the reference frequency f_0 (generally 1 Hz) and n is the frequency parameter, which is close to 1 and varies from region to region on the basis of heterogeneity of the medium (Aki, 1981).

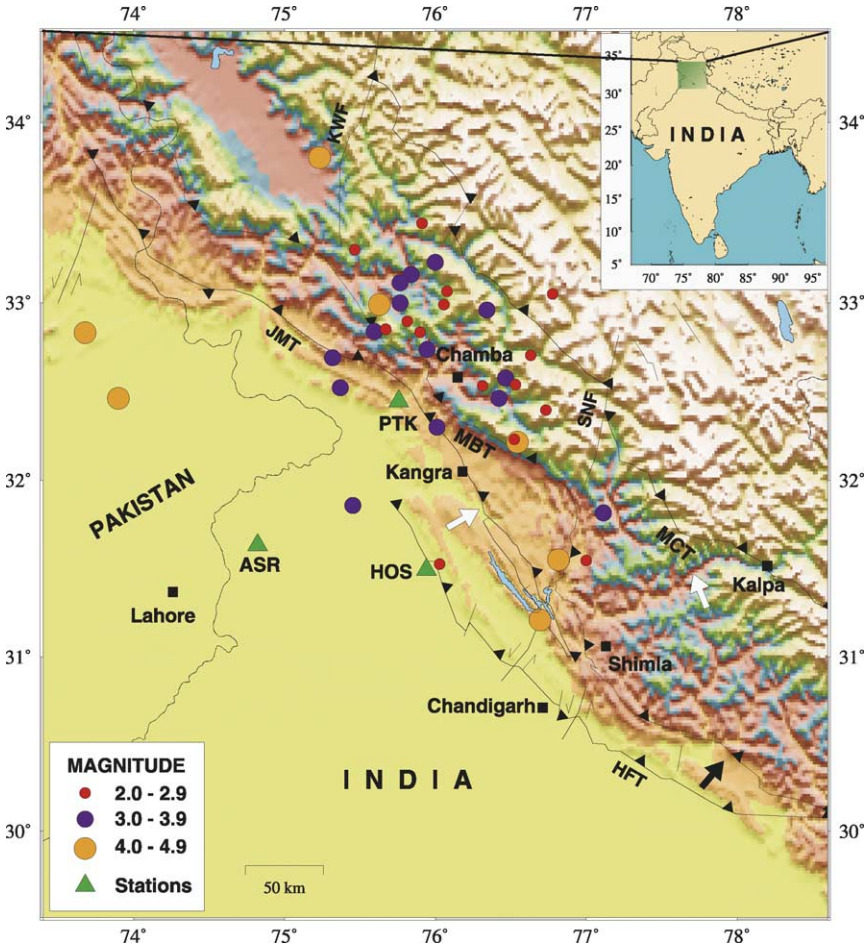

Fig. 1. General seismotectonic and topographical map of NW Himalayas and adjoining area. MCT: Main Central Thrust; MBT: Main Boundary Thrust; HFT: Himalayan frontal thrust; JMT: Jawalamukhi thrust; KWF: Kisatwar fault; SNF: Sundarnager fault; earthquake epicentres are plotted by circles, triangles represent the recording stations (PTK: Pathankot; HOS: Hoshiarpur; ASR: Amritsar) and cities are shown by squares.

This relation indicates that the attenuation of seismic waves with the passage of time (distance from source) is different for different frequencies. Hence, the seismic data is first bandpass filtered to calculate the attenuation. In the present study, the attenuation of S-coda wave is calculated at six central frequencies after bandpass filtered using Buterworth six pole filters as given in Table 2.

The amplitude of the coda wave at lapse time t seconds from the origin time for bandpass filtered seismogram at central frequency f is given by the attenuation method of the single back-scattering model as

$$A(f,t) \propto t^{-\alpha}\, \mathrm{e}^{-\pi f t/Q_c}$$

or

$$A(f,t) = K(f) t^{-\alpha}\, \mathrm{e}^{-\pi f t/Q_c} \quad (1)$$

where $K(f)$ is the coda source factor at frequency f, which is independent of time and radiation pattern, α is the geometrical spreading parameter having one value out of 1.0, 0.5 or 0.75 for body waves, surface waves or diffusive waves, respectively (Sato and Fehler, 1998), $Q_c(f)$ is the quality factor of coda waves. As coda waves are back-scattered body waves, therefore putting $\alpha = 1$ in Eq. (1) and taking the logarithm,

$$\ln\, A(f,t) = \ln\, K(f) - \ln(t) - \frac{\pi f}{Q_c(f)} t$$

or

$$\ln(A(f,t)t) = \ln\ K(f) - \frac{\pi f}{Q_c(f)}t \quad (2)$$

Hence Q_c is determined from the slope, b of least squares fit straight line plotting $\ln(A(f,t)t)$ versus t using the relation.

$$Q_c(f) = \frac{\pi f}{b} \quad (3)$$

The calculation of $Q_c(f)$ from the RMS values of amplitude with time is shown in Fig. 2 along with the plot of the coda window selected. According to Rautian and Khalturin (1978), the above relation is valid for lapse time greater than twice the S-wave travel time for avoiding the data of the direct S-wave and for validation of the model that the source of the earthquake and receiver are coincident. Sato (1977) introduced the source receiver offset in single scattering model so that the coda analysis begins after the arrival of the shear wave. In the present study, the time envelope for coda decay observation is taken at twice the time of the S-wave (2ts) from the origin time of the event.

4. Data analysis

The digital events data utilized for coda Q calculation were recorded during 1997–1999 at the regional seismograph network of three seismic stations by Earthquake Research Centre, Guru Nanak Dev University, Amritsar. As shown in Fig. 1, the first seismic station, PTK (Pathankot) is on the top of the Siwalik

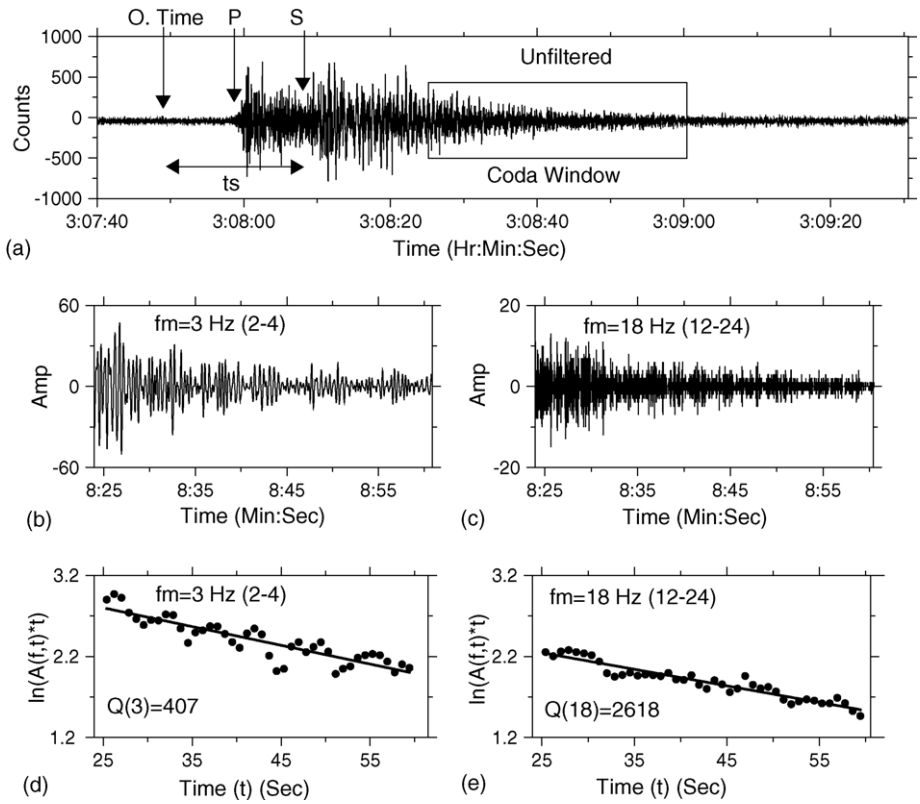

Fig. 2. Plot of event recorded at Pathankot station on 16/01/1999 from 66 km epicentral distance. (a) Unfiltered data trace with coda window, (b) and (c) bandpass filtered displacement amplitudes of coda window at 2–4 Hz and 12–24 Hz respectively, (d) and (e) the RMS amplitude values multiplied with lapse time along with best square fits of selected coda window at central frequencies of 3.0 and 18.0 Hz respectively. The Q_c is determined from the slope of best squareline. Abbrevations are: O. Time: Origin time; P: P-wave time; S: S-wave time.

hills, the second one, HOS (Hoshiarpur) is at Siwalik foothills, while third one, ASR (Amritsar) station is located on the Gangetic plain. The station PTK is situated on hard bedrock in the vicinity of high tectonic and seismic activity at high altitude. The station HOS is situated at alluvium near recent tectonic and moderate seismic activity, and the station ASR is on a thick alluvium of the Gangetic plain away from tectonic and seismic activities. All the stations were equipped with portable high quality three component short-period (1 Hz natural frequency) L4-3D seismometers of Mark products (USA) and high dynamic range 24 bit recording apparatus of REF TEK (USA). The instruments were setup to digitize the signal at 100 sps and an antiallising filter was applied to get the flat velocity spectrum between 1 and 40 Hz. During the given period, more than 300 seismic events were recorded from different epicentral ranges. Out of these, 36 local events with epicentral distance up to 200 km are analyzed for coda Q calculation. The epicenters of these selected events, the seismic stations, prominent discontinuities and the topography of the region are shown in Fig. 1.

A total of 126 seismograms of good S/N ratio are used in this study. The detailed epicentral information of seismic events is listed in Table 1, which indicates that the maximum events are recorded at PTK station while minimum events at HOS station. A few more local events are discarded due to low signal to noise ratio and other set criteria for coda Q calculation. We restrict the epicentral distance of PTK station up to 160 km for getting strong signal to noise ratio. The magnitude range of earthquakes is 2.1–4.8 and most of the events, nearly 60% are of shallow focal depth ($4 \leq h \leq 15$ km). The average focal depth of all the events is 23 km. Only four earthquakes have focal depth more than 35 km, in which the deepest earthquake is 82 km deep. Three deeper events are only from one small region, which is north to PTK station. On the basis of epicentral distance, 31 events of PTK station are further divided into three groups as $R \leq 55$ km as PTK1, $55 < R \leq 100$ km as PTK2 and $100 < R \leq 160$ km as PTK3. All the nine events of ASR station used here are from $100 \leq R \leq 200$ km of epicentral distance and in case of Hoshiarpur station both events taken in HOS group are from $50 \leq R \leq 100$ km epicentre range. Most of the seismic events are located between MBT and MCT bounded by two other transverse faults as the Sundernagar fault to the east and of same trend the Kistwar fault to the west. This region is very close to the PTK station in the northeast direction. The events of PTK station are also analyzed in three groups of focal depth as very shallow ($h \leq 15$ km) as PTK4, medium ($15 < h \leq 35$ km) as PTK5 and deeper ($35 < h \leq 82$ km) as PTK6 to observe the attenuation factor with varying depth of the lithosphere. Further, 18 events of Pathankot station lying between the MBT and MCT from 0° to 100° azimuths are analyzed separately in ACT group to see the effect of attenuation in seismically most active region.

The Q values are calculated through the CODAQ subroutine of SEISAN (Havskov and Ottemoller, 2003). The S-wave time is calculated through the P-wave time using $V_p/V_s = 1.74$. The lapse times are selected at 2ts to avoid the data of the direct S wave and to utilize the minimum possible sampling volume for Q_c values (Havskov et al., 1989). The observations by Roecker et al., 1982, Havskov et al., 1989, Gupta et al., 1998, Giampiccolo et al., 2002 from different regions of the world indicate increased value of Q_c with lapse time, which is due to greater penetration of waves in the deeper part where the attenuation is less. Therefore, eight window lengths are taken from 25 to 60 s with a variation of 5 s to estimate the attenuation at different lapse times for observing the effect with depth. At these window lengths all the seismograms are band pass filtered at central frequencies (f_m) of 1.5, 3.0, 6.0, 9.0, 12.0 and 18.0 Hz with bandwidths of 1.0, 2.0, 4.0, 6.0, 8.0 and 12.0, respectively. An increasing frequency band is used for increasing central frequency to avoid ringing and to take constant relative bandwidths for getting equal amount of energy into each band as suggested by Havskov and Ottemoller (2003). The RMS amplitude of the last 5 s data of lapse time window is divided by noise data of same length before the onset of the P wave to calculate the S/N ratio. All the seismograms having S/N ratio below 2 are rejected for better Q_c values. In the same manner the criteria of correlation coefficient ≥ 0.48 is applied to obtain reliable Q_c values. The comparison of the number of values selected for each frequency and lapse time to observe the average Q_c is described by the factor N in Table 2. The logarithm of product of RMS amplitude and lapse time is plotted against lapse time as shown in Fig. 2 for calculating Q_c from slope of the linear regression curve of $\ln(A(f, t)t)$ and t.

Table 1
Earthquake data used for CODAQ calculation

Sr. No.	Date (dd/mm/yy)	O. Time (hh:mm:ss)	Latitude (°N)	Longitude (°E)	Δ (km)	Depth (km)	Magnitude	Source
Station: Pathankot; latitude: 32.45°N; longitude: 75.76°E; elevation: 600 m								
$R \leq 55$								
1	01/07/98	22:50:51.4	32.691	75.318	49.4	19.5	3.5	IMD
2	05/07/98	22:33:36.7	32.852	75.675	54.7	10.0	2.4	IMD
3	05/07/98	23:04:21.8	32.837	75.596	45.9	12.0	3.0	IMD
4	31/07/98	02:16:14.5	32.522	75.372	37.1	6.0	3.6	IMD
5	28/09/98	00:21:02.6	32.737	75.947	36.9	15.0	3.1	IMD
6	06/11/98	14:29:34.5	32.299	76.010	28.8	34.0	3.8	IMD
7	21/02/99	15:14:56.5	32.833	75.898	44.9	10.0	2.1	IMD
8	22/03/99	20:31:17.7	32.894	75.813	49.9	5.0	2.2	IMD
9	28/07/99	10:42:52.7	32.533	76.313	53.0	10.0	2.5	IMD
Average					44.5	13.5		
$55 < R \leq 100$								
10	18/05/98	12:29:31.8	33.157	75.839	79.2	65.0	3.5	ISC
11	06/07/98	10:24:08.8	32.987	75.629	61.2	82.5	4.2	USGS
12	17/08/98	17:55:00.8	33.223	76.001	89.1	33.0	3.4	USGS
13	25/08/98	11:48:04.9	32.543	76.533	73.7	15.0	2.6	IMD
14	02/09/98	01:02:26.1	32.957	76.342	78.9	5.0	3.0	IMD
15	17/10/98	09:24:45.0	32.217	76.545	78.4	33.0	4.5	USGS
16	16/01/99	03:07:46.8	32.987	76.058	66.3	5.0	2.7	IMD
17	15/02/99	00:14:52.0	32.232	76.523	75.9	4.0	2.7	IMD
18	15/03/99	21:56:37.5	33.062	76.078	74.6	5.0	2.5	IMD
19	16/03/99	19:16:19.2	32.396	76.732	91.9	15.0	2.3	IMD
20	27/03/99	11:49:31.4	32.462	76.422	62.5	10.0	3.5	IMD
21	22/04/99	05:22:04.8	32.996	75.768	61.0	7.0	3.2	IMD
22	07/05/99	14:44:57.4	31.861	75.455	70.0	33.0	3.0	IMD
23	12/07/99	21:45:59.4	33.110	75.768	73.6	72.0	3.7	USGS
24	27/07/99	20:19:09.7	32.577	76.466	68.2	10.0	3.2	IMD
25	30/07/99	18:18:25.2	32.704	76.633	87.1	15.0	2.5	IMD
Average					74.5	25.6		
$100 < R \leq 160$								
26	23/12/97	04 15 04.9	33.805	75.234	158.0	33.0	4.0	ISC
27	25/04/98	18 15 50.8	31.533	76.028	104.0	30.0	2.3	IMD
28	28/09/98	21 17 01.0	31.551	76.995	153.0	22.0	2.2	IMD
29	11/01/99	01 30 26.1	31.820	77.115	146.0	5.0	3.5	IMD
30	08/05/99	20 59 17.4	33.442	75.912	111.0	15.0	2.7	IMD
31	31/07/99	13 02 25.8	33.046	76.777	116.0	15.0	2.2	IMD
Average					131.3	20.0		
Station: Amritsar; latitude: 31.64°N; longitude: 74.82°E; elevation: 218 m								
$100 \leq R \leq 202$								
1	29/07/97	09 43 35.8	32.831	73.680	171.0	10.0	4.8	USGS
2	29/07/97	18 00 18.2	31.554	76.817	189.0	33.0	4.7	USGS
3	13/08/97	23 10 15.1	31.211	76.694	184.0	33.0	4.2	USGS
4	21/02/98	19 08 04.3	33.292	75.466	193.0	15.0	2.6	IMD
5	24/03/98	04 25 42.9	32.462	73.901	126.0	42.5	4.0	USGS
6	01/07/98	22 50 51.4	32.691	75.318	126.0	19.5	3.5	IMD
7	05/07/98	23 04 21.8	32.837	75.596	152.0	12.0	3.0	IMD
8	28/09/98	21 17 01.1	31.551	76.995	202.0	30.0	2.2	IMD
9	17/10/98	09 24 45.0	32.217	76.545	175.0	33.0	4.5	USGS
Average					168.7	25.3		
Station: Hoshiarpur; latitude: 31.50°N; longitude: 75.94°E; elevation: 284 m								
$50 \leq R \leq 100$								
1	17/10/98	09 24 45.0	32.217	76.545	98.1	4.5	4.5	USGS
2	06/11/98	14 29 34.5	32.299	76.010	89.1	34.0	3.8	IMD
Average					93.6	14.75		

Table 2
Average quality factor at different frequencies and lapse times

Lapse time (s)	1.5 Hz (1–2) $Q_c \pm \sigma$	N	3 Hz (2–4) $Q_c \pm \sigma$	N	6 Hz (4–8) $Q_c \pm \sigma$	N	9 Hz (6–12) $Q_c \pm \sigma$	N	12 Hz (8–16) $Q_c \pm \sigma$	N	18 Hz (12–24) $Q_c \pm \sigma$	N
25	131 ± 36	69	335 ± 69	42	693 ± 148	38	1160 ± 126	31	1483 ± 198	32	2299 ± 397	16
30	170 ± 44	74	402 ± 51	36	795 ± 149	48	1305 ± 168	45	1562 ± 214	31	2593 ± 392	23
35	178 ± 48	73	425 ± 96	44	848 ± 131	53	1458 ± 248	51	1774 ± 235	36	2754 ± 399	30
40	202 ± 63	73	522 ± 115	51	936 ± 172	64	1555 ± 253	56	1944 ± 219	41	3027 ± 367	32
45	216 ± 66	67	526 ± 106	53	1045 ± 192	64	1635 ± 244	55	2138 ± 233	45	3112 ± 350	31
50	239 ± 72	71	569 ± 127	47	1113 ± 164	59	1765 ± 270	55	2211 ± 249	41	3111 ± 397	30
55	266 ± 82	71	637 ± 193	55	1262 ± 171	52	1716 ± 235	46	2303 ± 238	37	2953 ± 442	29
60	285 ± 95	68	656 ± 177	51	1352 ± 208	52	1715 ± 221	43	2225 ± 238	35	2869 ± 335	27

5. Results

The quality factor, Q_c has been estimated to assess the effect of tectonic and seismic activity in the NW Himalayas. The data is analyzed in nine groups to observe the attenuation factor at different epicentral range, depth range and for a small high seismic active region. The information of the analyzed earthquakes is given in Table 1. The average Q_c values of the region for all lapse times and frequencies are mentioned in Table 2 and Q_0 along with n are given in Table 3. The dimensions of ellipsiodal volume for different groups are in Table 4. Fig. 3 shows the comparison of Q_0 (quality factor at 1 Hz) and frequency parameter, n for all the groups. Fig. 4 shows the plot of Q_c and central frequencies with linear regression fit for all the stations. Average values of Q_0, Q_c and frequency parameter, n are plotted in Fig. 5, while $Q_c{}^{-1}$ values of NW Himalayas are compared with other regions of the world in Fig. 6. The detailed results of these figures and tables are discussed below and in the next section.

In the single scattering model the estimated attenuation of coda wave is the average decay of amplitude of back-scattered waves on the surface of ellipsoid volume having earthquake source and station as foci (Pulli, 1984). On this basis the approximate ellipsoidal volume for nine groups of seismic events is estimated, which shows average attenuation properties of the region. The observed Q_c reflects the average attenuation properties of the volume of ellipsoid at an average depth, $h = h_{av} + a2$, where h_{av} is the average focal depth of the events and $a2 = \sqrt{a1^2 - \Delta^2}$ is the small semi axis of the ellipsoid for Δ as average epicentral distance (Pulli, 1984; Havskov et al., 1989; Canas et al., 1995). The large semi-axis of the ellipsoidal volume is $a1 = ct/2$ for lapse time t and velocity c of the Lg wave ($c = 3.5$ km/s). The average lapse time is taken as

$$t = t_{start} + \frac{W}{2}$$

where t_{start} is the starting time of the coda window and W is the coda window length. The depths calculated for the ellipsoidal volume for different groups of data are given in Table 4.

The Pathankot station is in the vicinity of high seismic and tectonic activity. The data recorded at this station is analyzed in detail to differentiate the attenuation factor laterally, vertically and seismotectonically.

Table 3
Q_0 (quality factor at 1 Hz) and n values for all the stations

Lapse time (s)	Pathankot							
	$R \leq 55$		$55 < R \leq 100$		$100 < R \leq 160$		Average	
	Q_0	n	Q_0	n	Q_0	n	Q_0	n
25	77	1.18	87	1.13	82	1.24	82.00	1.18
30	81	1.18	98	1.13	100	1.17	93.00	1.16
35	90	1.18	117	1.11	131	1.03	112.67	1.11
40	100	1.18	139	1.07	141	1.06	126.67	1.10
45	98	1.21	158	1.04	133	1.15	129.67	1.13
50	103	1.22	169	1.04	167	1.02	146.33	1.09
55	119	1.17	204	0.94	195	0.95	172.67	1.02
60	121	1.17	214	0.94	234	0.85	189.67	0.99

	Amritsar ($100 \leq R \leq 202$)		Hoshiarpur ($50 \leq R \leq 100$)		Average of all stations ($R \leq 202$)	
	Q_0	n	Q_0	n	Q_0	n
25	109	1.05	69	1.26	86.67	1.16
30	168	0.93	115	1.11	125.33	1.07
35	174	0.97	98	1.21	128.22	1.10
40	207	0.95	125	1.15	152.89	1.07
45	231	0.92	119	1.18	159.89	1.08
50	235	0.94	155	1.11	178.78	1.05
55	265	0.89	197	0.99	211.56	0.97
60	249	0.94	225	0.92	221.22	0.95

PTK1 group contains the data of Pathankot station for epicentral distance less than 55 km. In this group nine events of high S/N ratio and greater correlation coefficients are analyzed. The average focal depth of the earthquakes is 13.5 km and the average epicentral distance is 44.5 km. As shown in Fig. 1, the region of this data group is in and around sub-Himalayas containing the MBT and the JMT as major tectonic features. Fig. 3(a) indicates the low values of Q_0 for this group as compared to other data groups. Its variation with lapse time is small for 25–50 s window lengths. After 50 s there is some increase in the Q_0 value, which indicates that the deeper region is homogenous with some drastic change. The effect of the frequency parameter is given in Fig. 3(b), which shows that the frequency parameter effect to this group of data is high. The value of this parameter is almost constant for all lapse times with standard deviation merely 0.02. The average quality factor at 1.5 Hz is 144.5, while its value at 18 Hz is 2829. The Q_c frequency relationship for this data is $98.6f^{1.19}$ and the depth of the ellipsoidal volume is 76.6 km. The low value of Q_0 and nearly

Table 4
The maximum depth of ellipsoidal volume

Data group	Average Δ	Average h_{av}	t	$a1 = ct/2$ $c = 3.5$ km/s	$a2 = \sqrt{a1^2 - \Delta^2}$	Depth $h = h_{av} + a2$
PTK1	44.5	13.5	44.10	77.2	63.1	76.6
PTK2	74.5	25.6	69.93	122.4	97.1	122.7
PTK3	131.3	20.0	103.20	180.6	124.0	144.0
ASR	168.7	25.3	120.98	211.7	127.9	153.2
HOS	93.6	14.8	75.80	132.7	94.0	108.7
PTK4	71.8	9.7	66.01	115.5	90.5	100.2
PTK5	91.3	29.7	72.96	127.7	89.3	119.0
PTK6	71.3	73.2	77.05	134.8	114.4	187.6
ACT	68.5	13.7	65.10	113.9	91.0	104.7

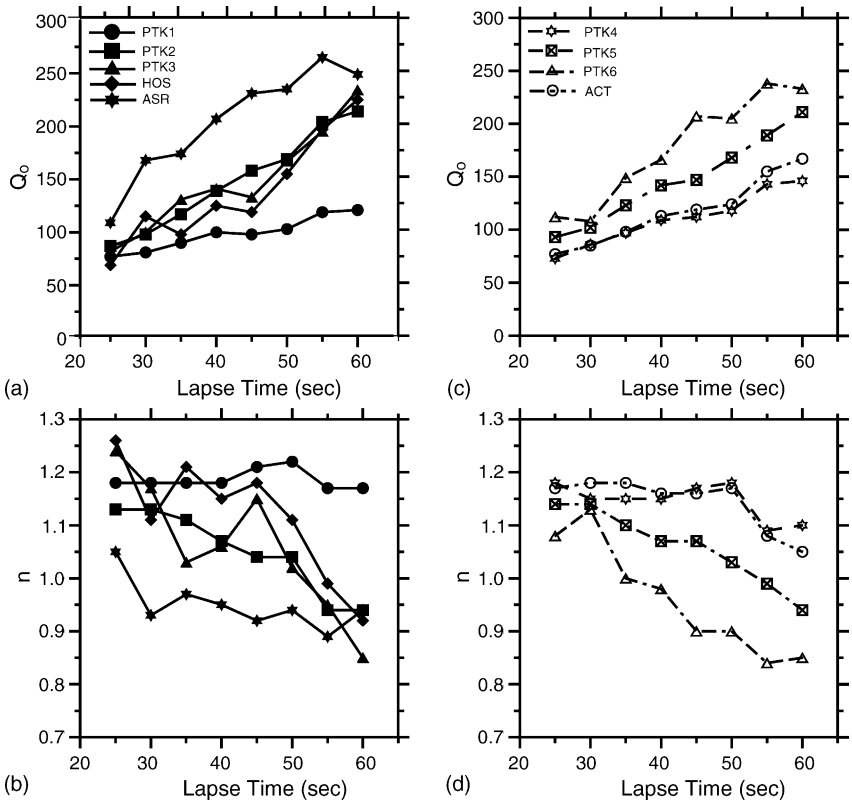

Fig. 3. Plots of Q_0 (quality factor at 1 Hz) and n (frequency parameter) with lapse time for different groups of data. PTK1 ($R \leq 55$), PTK2 ($55 < R \leq 100$), PTK3 ($100 < R \leq 160$) are different epicentre ranges for Pathankot; ASR, Amritsar; HOS, Hoshiarpur; PTK4 ($h < 15$), PTK5 ($15 < h \leq 35$), PTK6 ($35 < h \leq 82$) are data groups of different focal depths, ACT, Active region data. Q_0 and n are plotted with lapse time in (a), (b), (c) and (d) for these data groups.

constant high value of frequency parameter indicate that the upper lithosphere around this data group is seismically active and contains more heterogeneities.

The station ASR is located on the alluvium which is far from the Himalayas. The seismic sources are relatively distant from this station, the data of nine events in epicentre range of 100–200 km are analyzed but due to low S/N ratio about 40% values of these events are rejected. The Q_0 values of this station are relatively high and frequency parameter is low for all the lapse times. Fig. 3(a) and (b) show that the values of these parameters are reversed as compared to the values of PTK1 group. The frequency dependent relationship is $205f^{0.95}$, the high Q_0 value of 205 and low n value of 0.95 show that the region is intermediate active and less heterogeneous. As mentioned in tectonic setting and seismic activity, the recent geological features and neotectonic activity (Fig. 1) near to PTK station may be responsible for high attenuation in PTK1 group, while this attenuation is comparatively low for ASR data having older geological features and less deformations.

The data analyzed in the PTK2, PTK3 and HOS groups covered almost the same area for the scattered waves. The data of PTK3 group is of shallow focus having more epicentral distance and due to low magnitudes and high attenuation around this station, the S/N ratio is low, therefore most of the seismic data is rejected due to set criteria. The frequencies higher than 12 Hz are so severely attenuated that only 10% of the calculations for central frequency 12 Hz are chosen and all the data above 12 Hz is rejected. In these groups most of the data is from the subduction zone having the subcrustal deformation along HFT, JMT and MBT tectonic features. The scattered waves are from two

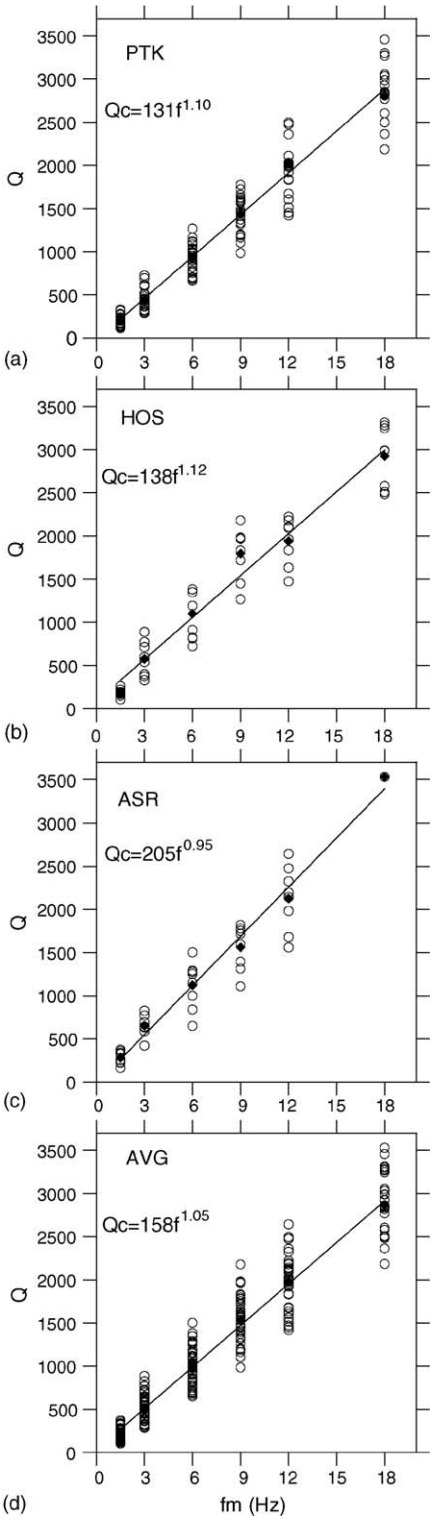

different regions, the region to the north and northeast of the stations is seismic and tectonically active while the southwestern part is a foredeep covered with Gangetic alluvium and is less deformed. The attenuation of S-coda mainly for 1 Hz central frequency of these groups is less as compared to PTK1 but more than that of ASR. The reason may be the epicentral range, seismic activity, tectonic activity and geological features. It is clear from Fig. 3(a) and (b) that the Q_0 for these data groups increases and n decreases with the lapse time. This shows that the upper part of the lithosphere is heterogeneous and seismically active. The frequency parameter for HOS group is higher for all the lapse times, which indicates that the upper lithosphere around this station is more heterogeneous. This may be due to greater deformation of the region through recent Himalayan orogeny e.g. HFT. The calculated Q_0 and n values of all the stations are given in Table 3.

The data of Pathankot station is further analyzed at different focal depths in PTK4, PTK5 and PTK6 data groups. Moreover, the data of high seismic active sub-region of the current study towards the northeast of Pathankot station are analyzed in the ACT (active region) group. The Q_0 and n values of these data groups are shown in Fig. 3(c) and (d). In all the groups the Q_0 increases with increasing lapse time but its value and the increment is more as focal depth increases. The patterns of Q_0 is more or less similar for PTK4 and ACT data groups with slightly more values for ACT for lapse time more than 50 s. The variation of n value is less for PTK4 and ACT. Its value is high and almost constant upto lapse time 50 s and after that it drops, which is the clear indication that upper lithosphere is more heterogeneous. The data of PTK5 and PTK6 shows that n value decreases with the lapse time and focal depth. The depth of ellipsoidal volume for these data groups is given in Table 4. These results indicate that upper lithosphere is heterogeneous and coda attenuation is effective with seismic activity.

The variation in Q_0 and n of all the groups indicates that the area of the northern part of the region seems

Fig. 4. Plots of quality factors and central frequencies for all stations with linear regression frequency dependent relationship, $Q_c = Q_0 f^n$. (a) Q_c with f_m (central frequency) for all epicentre distances of Pathankot ($Q_c = 136f^{1.07}$), (b) Q_c with f_m for Hoshiarpur ($Q_c = 138f^{1.12}$), (c) Q_c with f_m for Amritsar ($Q_c = 205f^{0.95}$), (d) Average Q_c with f_m for all the stations ($Q_c = 158f^{1.05}$).

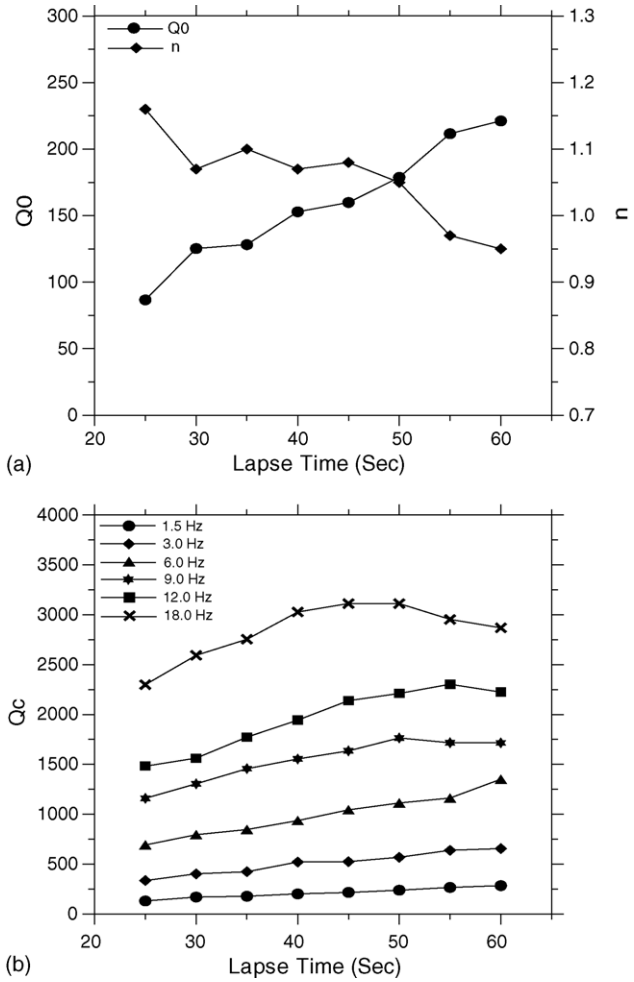

Fig. 5. Plot of average values of Q_c, Q_0 and n with lapse time for all the stations. (a) average Q_0 and n with lapse time, (b) Average Q_c with lapse time at different central frequencies.

to be more active and heterogeneous than the southern part. But the upper lithosphere near the current deformation (conjunction of Himalayas and the alluvium) is more heterogeneous. The average Q_c along with individual values of all the stations is plotted in Fig. 4(a–d). These figures show the pattern of quality factor with central frequencies and best least square fits are interpolated to get the frequency dependent relationship of quality factor. The average frequency dependent relationship for NW Himalayan region is $158f^{1.05}$. The variation of Q_c with frequency, Q_0 and n of these stations is due to the difference in geological formations, seismic activity and tectonic activity near these stations. The average Q_c of the region is frequency dependent but its effect is more towards north and northeast, where the tectonic and seismic activity is more.

6. Discussion

The trend of quality factor, Q_0 and frequency parameter, n for the data of PTK1, PTK4 and ACT (active region) is similar for all the lapse times. The data of these groups have different sources near Pathankot station but the maximum depth of ellipsoidal volume is almost same around 100 km. These values indicate that the upper lithosphere near MBT and MCT

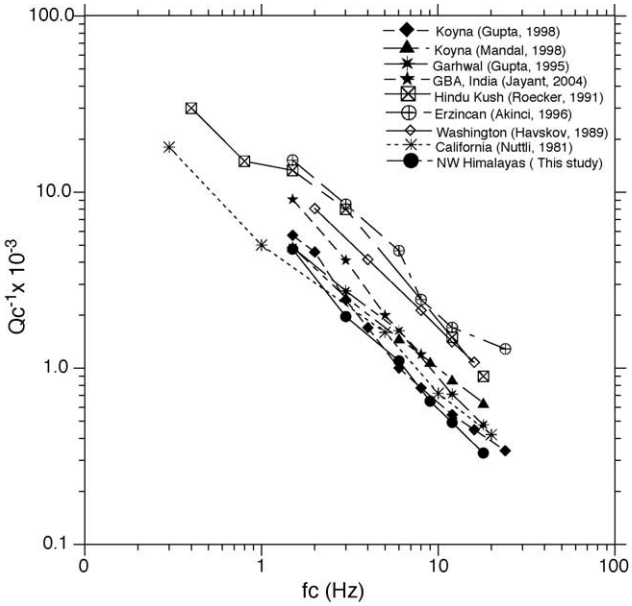

Fig. 6. Comparison of coda-Q_c of NW Himalayan region with reported coda-Q_c of other regions of the world.

is seismically active and highly heterogeneous. Along with these groups the data of HOS group indicate that frequency parameter is more effective for the upper lithosphere. This low value of Q_0 and high frequency parameter has been suggested due to more seismic activity and heterogeneities in the upper part of lithosphere in brittle-ductile zone, which is the effect of tectonic stress loading in brittle-ductile transition (Aki, 2003). If we compare the values of these groups with the values of ASR data then the results are not similar and we can say that the foredeep Gengetic plain covered with alluvium is less active and less heterogeneous. Recently Mandal et al. (2004) have studied the coda attenuation factor in the epicentral region of devastating 2001 Bhuj earthquake using aftershocks data to estimate Q_c effect with seismicity and heterogeneity. Their findings reveal low Q_0 values in aftershock zone as compared to adjoining regions. This implies that the attenuation is more near seismically active and heterogeneous region and indicates high value of frequency parameter with heterogeneous upper lithosphere and homogeneous deeper part.

As shown in Fig. 5(a) the trend of average Q_0 with lapse time shows that its value increases with lapse time. If we neglect the multiple scattering effect then it shows that upper lithosphere is more active. The trend of n first decreases then becomes somewhat constant for longer lapse times and after that it decreases more for much longer lapse times, which reflects that uppermost crust is more heterogeneous. The increase in Q_c with lapse time (Fig. 5(b)) is the increase of Q_c with depth since longer the coda window, the larger will be the sample of ellipsoidal volume of the lithosphere (Table 4). The same trend of Q_c with lapse time has been observed by Roecker et al., 1982; Ibanez et al., 1990; Akinci et al., 1994; Gupta et al., 1998. There may be the effect of multiple scattering for longer lapse times (Gao et al., 1983), which we have neglected by taking single scattering model. Sato (1988) has observed that the multiple scattering effect is insignificant and according to Gao et al. (1983) it is not so much effective for lapse times less than 100 s. In the present study, we have analyzed the data for lapse time upto 60 s and thus the effect of multiple scattering may not be very much significant. We have also observed that the effect of magnitude variation for events near to station is insignificant for coda attenuation.

The difference in Q_c values between Amritsar (ASR) and other two stations is greater, which may be considered probably due to real crustal differences in terms of coda Q (Fig. 4). This indicates that the average attenuation properties and the scatters in the

study area have different pattern. The attenuation of seismic energy is more towards the Himalayan belt but comparatively less towards the Gangetic plains. This variation may be due to differences in seismotectonic, geotectonic, epicentral distance and focal depths in the subregions. To observe the effect of focal depths the events are divided in three groups but the number of events of shallow focus depths were more (65%) and deep focus depth less (10%). The estimated relation of Q_c gives an average strong frequency dependent relationship of $Q_c = Q_0 f^n$, with mean value of n as 1.05 and varies for different parts of the region. The quality factor is also lapse time dependent and from 25 to 50 s window length, its value increases with lapse time for all the frequencies (Fig. 5(b)). This means that for ellipsoidal volumes upto a tentative depth of 85 km the attenuation decreases with depth and medium homogeneity increases. After 50 s lapse time there is still a small increment of Q_c for lower frequencies (less than 10 Hz) but no variation for higher frequencies, indicating homogeneous lower lithosphere. We also tried to find out the variation in coda quality factor laterally and vertically to observe the subcrustal heterogeneities and seismotectonics through different groups of data. The results show the variation for different parts but these variations cannot be taken as sharp division of the region because in the S–S back-scattering model the scattering is the average property of the region. Also all the stations did not record enough data used for Q_c calculation and the maximum selected events are clustered in a small subregion. Therefore, to observe all these effects in detail, we may require more data. High dependence of Q_c with frequency than its low value at 1 Hz indicates more effect of heterogeneities and tectonics in the upper crust as compared to seismic activity. The local variation in Q_0 values is probably controlled by local geology of the region.

The coda attenuation, ${Q_c}^{-1}$ values estimated at different frequencies in this study, are compared with other tectonic and seismic active regions of the world in Fig. 6. The ${Q_c}^{-1}$ values of this region are comparable to other Indian regions but less than most of the other available values of the world. The coda attenuation of this region is similar to California as given by Nuttli (1981). Parvez et al. (2001) have also observed that the attenuation law of NW Himalayas is comparable to other seismogenic zones in the world and very similar to California and Japan. Our results also agree with other Indian active regions but are less than other observed active regions of the world. The frequency parameter of this region is greater compared to the other regions, which indicates that the upper lithosphere of the region is more heterogeneous. The frequency parameter is nearly constant for data groups having epicentre distances less than 55 km, focal depths less than 15 km and active subregion as given in Fig. 3. Also in some other regions of the world no significant variation of frequency parameter has been observed for smaller lapse time windows and shallow focus depths (e.g. Ibanez et al., 1990; Akinci et al., 1994). The attenuation properties of the Indian lithosphere have been estimated earlier by coda Q methods for some regions by Gupta et al., 1995 for Garhwal Himalayas, Mandal and Rastogi, 1998 for Koyna region, Gupta et al., 1998 for Koyna region, Tripathi and Ugalde, 2004 for southern Indian region and Mandal et al., 2004 for Kutch area. It is quite clear from Fig. 6 that the coda Q^{-1} values observed by this study are comparable to other Indian regions but more sensitive to frequency, which shows that this region is more heterogeneous as compared to other parts of the country.

7. Conclusion

The estimated coda Q value of NW Himalayas indicates that the attenuation is greater towards high tectonic and seismic active areas. The estimated average frequency dependent relationship of the region is $158f^{1.05}$, while this relationship varies from $138f^{1.1}$ for mountains and its foothills to $205f^{0.95}$ for the plains. The observed quality factor is strongly dependent on frequency and lapse time, which indicates that the upper lithosphere, is more heterogeneous and seismotectonically active, while the lower lithosphere is homogeneous and relatively less active. The seismic data for the regions of epicentral distances less than 55 km, focal depths less than 15 km and highly seismic active subregions of current study indicate low values of Q_0 and high values of frequency parameter. The frequency parameter of these selected data groups is high and almost constant upto 50 s lapse time window length, which indicates that upper lithosphere is highly heterogeneous. The frequency dependent quality factor indicates that the seismic energy of high frequency waves is attenuated more in upper lithosphere than in

the lower lithosphere. The coda attenuation factor of NW Himalayas is comparable to other seismic active regions of India but the frequency parameter is somewhat more sensitive than the other regions. The trend of coda energy attenuation is similar to other seismic and tectonic active regions of the World. The subregional variation of Q_0 and frequency parameter indicates that seismic activity and heterogeneity of the lithosphere affect the attenuation behaviour of seismic waves.

Acknowledgement

We are very thankful to Prof. K. Aki for his encouragement and constructive suggestions to improve the quality of the manuscript. We thank Dr. Gangan Prathap, Scientist-in-Charge, CMMACS for his permission and to provide the facilities to complete this work. We also thank the Department of Science and Technology, Government of India to provide the fellowship to N.K. under DST project R-0-134.

References

Aki, K., 1969. Analysis of the seismic coda of local earthquakes as scattered waves. J. Geophys. Res. 74, 615–631.

Aki, K., Chouet, B., 1975. Origin of the coda waves: source, attenuation and scattering effects. J. Geophys. Res. 80, 3322–3342.

Aki, K., 1981. Source and scattering effects on the spectra of small local earthquakes. Bull. Seismol. Soc. Am. 71, 1687–1700.

Aki, K., 2003. Seismology of earthquake and volcanic prediction, in: Proceedings of the Seventh Workshop on Non-Linear Dynamics and Earthquake Prediction, The Abdus Salam International Centre for Theoretical Physics, Trieste, Italy, H4.SMR/1519-10.

Akinci, A., Taktak, A.G., Ergintav, S., 1994. Attenuation of coda waves in Western Anatolia. Phys. Earth Planet Inter. 87, 155–165.

Canas, J.A., Pujades, L., Badal, J., Payo, G., de Miguel, F., Vidal, F., Alguacil, G., Ibanez, J., Morales, J., 1991. Lateral variation and frequency dependence of coda-Q in the southern part of Iberia. Geophys. J. Inter. 107, 57–66.

Canas, J.A., Pujades, L., Blanco, M.J., Soler, V., Carracedo, J.C., 1995. Coda-Q distribution in the Canary Islands. Tectonophysics 246, 245–261.

Dubey, A.K., Misra, R., Bhakuni, S.S., 2001. Eratic shortening from balanced cross-sections of the western Himalayan foreland basin: causes and implication for basin evolution. J. Asian Earth Sci. 19, 765–775.

Gao, L.S., Lee, L.C., Biswas, N.N., Aki, K., 1983. Comparison of the effects between single and multiple scattering on coda waves for local earthquakes. Bull. Seismol. Soc. Am. 73, 377–389.

Giampiccolo, E., Tusa, G., Langer, H., Gresta, S., 2002. Attenuation in southeastern Sicily (Italy) by applying different coda methods. J. Seismol. 6, 487–501.

Gupta, S.C., Singh, V.N., Kumar, A., 1995. Attenuation of coda waves in the Garhwal Himalayas. India. Phys. Earth Planet Inter. 87, 247–253.

Gupta, S.C., Teotia, S.S., Gautam, N., 1998. Coda *Q* estimates in the Koyna region, India. Pure Appl. Geophys. 153, 713–731.

Havskov, J., Ottemoller, L., 2003. SEISAN: The Earthquake Analysis Softwares for Windows, Solaris and Linux, Version 8.0. Institute of Solid Earth Physics, University of Bergen, Norway.

Havskov, J., Malone, S., McClurg, D., Crosson, R., 1989. Coda Q for the state of Washington. Bull. Seismol. Soc. Am. 79, 1024–1038.

Ibanez, J.M., Del Pezzo, E., De Miguel, F., Herraiz, M., Alguaicil, G., Morales, J., 1990. Depth dependent seismic attenuation in the Granada zone (southern Spain). Bull. Seismol. Soc. Am. 80, 1232–1244.

Jin, A., Aki, K., 1988. Spatial and temporal correlation between coda Q and seismicity in China. Bull. Seismol. Soc. Am. 78, 741–769.

Jin, A., Aki, K., 1989. Spatial and Temporal correlation between coda Q^{-1} and seismicity and its physical mechanism. J. Geophys. Res. 94, 14041–14059.

Latchman, J.L., Ambeh, W.B., Lynch, L.L., 1996. Attenuation of seismic waves in the Trinnidad and Tobago area. Tectonophysics 253, 111–127.

Mandal, P., Rastogi, B.K., 1998. A frequency-dependent relation of coda Q_c for Koyna-Warna region. India. Pure Appl. Geophys. 153, 163–177.

Mandal, P., Jainendra, Joshi, S., Kumar, S., Bhunia, R., Rastogi, B.K., 2004. Low coda Q_c in the epicentral region of the 2001 Bhuj earthquake of M_w 7.7. Pure Appl. Geophys. 161, 1635–1654.

Mitchell, B., 1981. Regional variation and frequency dependence of Q_β in the crust of the United States. Bull. Seismol. Soc. Am. 71, 1531–1538.

Ni, J., Barazangi, M., 1984. Seismotectonics of the Himalayan collision zone: geometry of the underthrusting Indian plate beneath the Himalayas. J. Geophys. Res. 89, 1147–1163.

Nuttli, O.W., 1981. Similarities and differences between western and eastern United States earthquakes, and their consequences for earthquake engineering. In: Beavers, J.E. (Ed.), Proceedings of the Conference on Earthquakes and Earthquake Engineering: the Eastern United States. vol. 1. Ann Arbor Science Publishers, Inc., Ann Arbor, Michigan, pp. 25–27.

Parvez, I.A., Gusev, A.A., Panza, G.F., Petukhin, A.G., 2001. Preliminary determination of interdependence among strong-motion amplitude, earthquake magnitude and hypocentral distance for the Himalayan region. Geophys. J. Int. 144, 577–596.

Peng, J.Y., Aki, K., Lee, W.H.K., Chouet, B., Johnson, P., Marks, S., Newberry, J.T., Ryal, A.S., Stewart, S.W., Tottingham, D.M., 1987. Temporal change in coda Q associated with 1984 Round Valley earthquake in California. J. Geophys. Res. 92, 3507–3536.

Pujades, L., Canas, J.A., Egozcue, J.J., Puigvi, M.A., Pous, J., Gallart, J., Lana, X., Casas, A., 1991. Coda Q distribution in the Iberian Peninsula. Geophys. J. Int. 100, 285–301.

Pulli, J.J., 1984. Attenuation of coda waves in New England. Bull. Seismol. Soc. Am. 74, 1149–1166.

Rao, N.P., Kumar, M.R., Tsukuda, T., 2003. Current deformation of the Himalaya-Tibet-Burma seismic belt: inferences from seismic activity and strain rate analysis. J. Geodyn. 36, 485–496.

Rautian, T.G., Khalturin, V.I., 1978. The use of coda for determination of the earthquake source spectrum. Bull. Seismol. Soc. Am. 68, 923–948.

Roecker, S.W., Tucker, B., King, J., Hartzfield, D., 1982. Estimates of *Q* in Central Asia as a function of frequency and depth using the coda of locally recorded earthquakes. Bull. Seismol. Soc. Am. 72, 129–149.

Sato, H., 1977. Energy propagation including scattering effects: single isotropic approximation. J. Phys. Earth 25, 27–41.

Sato, H., 1988. Fractal interpretation of the linear relation between logarithms of maximum amplitude and hypocentral distance. Geophy. Res. Lett. 15, 373–375.

Sato, H., Fehler, M., 1998. Seismic Wave Propagation and Scattering in the Heterogeneous Earth. AIP Press/Springer-Verlag, New York, pp. 1–308.

Singh, S.K., Herrmann, R.B., 1983. Regionalization of crustal coda Q in the continental United States. J. Geophys. Res. 88, 527–538.

Su, F., Aki, K., 1986. Spatial and temporal variation in coda Q^{-1} associated with the North Palm Springs earthquake of 1986. Pure Appl. Geophys. 133, 23–52.

Tripathi, J.N., Ugalde, A., 2004. Regional estimation of Q from seismic coda observation by the Gauribidanur seismic array (southern India). Phys. Earth Planet Inter. 145, 115–126.

Wu, R.S., 1985. Multiple scattering and energy transfer of seismic waves-seperation of scattering effect from intrinsic attenuation-I. Theoretical modelling, Geophys. J.R. Astr. Soc. 82, 57–80.

Wu, R.S., Aki, K., 1988. Multiple scattering and energy transfer of seismic waves-separation of scattering effect from intrinsic attenuation II. Application of the theory to Hindu-Kush region. Pure Appl. Geophys. 128, 49–80.

Zelt, B.C., Dotzev, N.T., Ellis, R.M., Roger, G.C., 1999. Coda *Q* in southwestern British Columbia. Can. Bull. Seismol. Soc. Am. 89, 1083–1093.